Science of the Total Environment 773 (2021) 145111

Contents lists available at ScienceDirect

Science of the Total Environment

journal homepage: www.elsevier.com/locate/scitotenv

Enzymatic degradation of polyethylene terephthalate nanoplastics analyzed in real time by isothermal titration calorimetry

Kristina Vogel [a,b], Ren Wei [c,*], Lara Pfaff [c], Daniel Breite [d], Hassan Al-Fathi [a], Christian Ortmann [e], Irina Estrela-Lopis [f], Tom Venus [f], Agnes Schulze [d], Hauke Harms [a], Uwe T. Bornscheuer [c], Thomas Maskow [a,*]

[a] Department of Environmental Microbiology, Helmholtz-Centre for Environmental Research – UFZ, Permoserstraße 15, D-04318 Leipzig, Germany
[b] Institute for Drug Discovery, Leipzig University Medical School, Leipzig University, Bruederstr, 34, D-04103 Leipzig, Germany
[c] Department of Biotechnology and Enzyme Catalysis, Institute for Biochemistry, University of Greifswald, Felix-Hausdorff-Str. 4, D-17487 Greifswald, Germany
[d] Leibniz Institute of Surface Engineering (IOM), Permoserstraße 15, D-04318 Leipzig, Germany
[e] TA Instruments, D-65760 Eschborn, Germany
[f] Institute for Medical Physics and Biophysics, Medical Faculty, Leipzig University, Härtelstr, 16-18, D-04107 Leipzig, Germany

HIGHLIGHTS

- Calorimetric method revealed the kinetics and degree of nanoplastic degradation.
- The exact enthalpy of ester bond cleavage in nanoplastic determined.
- Experimentally obtained thermal data validated the degradation kinetics.
- A two-step mechanism for biodegradation of nanoplastic confirmed.
- Polymer breakdown produced more heat than the adsorption of biocatalysts.

GRAPHICAL ABSTRACT

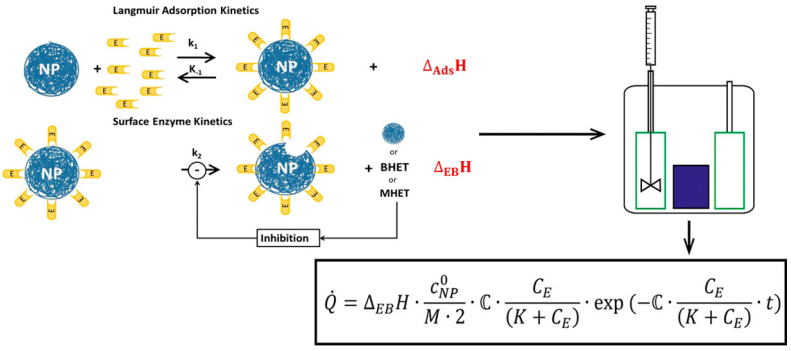

ARTICLE INFO

Article history:
Received 15 September 2020
Received in revised form 6 January 2021
Accepted 6 January 2021
Available online 3 February 2021

Editor: Fang Wang

Keywords:
Biothermodynamics
Cutinase
Heat balance
Surface adsorption
Thermokinetic model
PET

ABSTRACT

Plastics are globally used for a variety of benefits. As a consequence of poor recycling or reuse, improperly disposed plastic waste accumulates in terrestrial and aquatic ecosystems to a considerable extent. Large plastic waste items become fragmented to small particles through mechanical and (photo)chemical processes. Particles with sizes ranging from millimeter (microplastics, <5 mm) to nanometer (nanoplastics, NP, <100 nm) are apparently persistent and have adverse effects on ecosystems and human health. Current research therefore focuses on whether and to what extent microorganisms or enzymes can degrade these NP. In this study, we addressed the question of what information isothermal titration calorimetry, which tracks the heat of reaction of the chain scission of a polyester, can provide about the kinetics and completeness of the degradation process. The majority of the heat represents the cleavage energy of the ester bonds in polymer backbones providing real-time kinetic information. Calorimetry operates even in complex matrices. Using the example of the cutinase-catalyzed degradation of polyethylene terephthalate (PET) nanoparticles, we found that calorimetry (isothermal titration calorimetry-ITC) in combination with thermokinetic models is excellently suited for an in-depth analysis of the degradation processes of NP. For instance, we can separately quantify i) the enthalpy of surface adsorption $\Delta_{Ads}H = 129 \pm 2$ kJ mol^{-1}, ii) the enthalpy of the cleavage of the ester bonds $\Delta_{EB}H = -58 \pm 1.9$ kJ mol^{-1} and the apparent equilibrium constant of the enzyme substrate complex $K = 0.046 \pm 0.015$ g L^{-1}. It could be determined that the heat production of PET NP degradation depends to 95% on the reaction heat and only to 5% on the adsorption heat. The fact that the percentage of cleaved ester bonds ($\eta =$

* Corresponding authors.
E-mail addresses: ren.wei@uni-greifswald.de (R. Wei), Thomas.Maskow@ufz.de (T. Maskow).

https://doi.org/10.1016/j.scitotenv.2021.145111

12.9 ± 2.4%) is quantifiable with the new method is of particular practical importance. The new method promises a quantification of enzymatic and microbial adsorption to NP and their degradation in mimicked real-world aquatic conditions.

1. Introduction

Plastic litter poses a serious risk to the health of ecosystem and humans (Rochman et al., 2013; Wright and Kelly, 2017). As a result of the increasing global production of plastics, which has reached 359 million metric tons p.a. excluding synthetic fibers in 2018 (PlasticsEurope, Plastics - the Facts 2019), efficient waste disposal measures are urgently needed for the sustainable treatment of the equivalent amount of plastic waste. Current estimations assume that only 9% of the plastic waste was recycled worldwide in 2015 (Geyer et al., 2017). A tremendous amount of improperly or untreated plastic waste, hence, enters and accumulates persistently in the natural environment including the oceans (Jambeck et al., 2015; Lebreton et al., 2017; Worm et al., 2017) where larger plastic debris are fragmented into small particles called microplastics (<5 mm) and nanoplastics (NP, <100 nm). The latter often originate from the former by fragmentation as a result of both abiotic (e.g., mechanical abrasion, UV radiation) and biotic (e.g., ingestion by krill) effects (Dawson et al., 2018; Wagner and Reemtsma, 2019), instead of being degraded to harmless end products. Potential risks of microplastics to the environment and human health have been intensively studied in recent years but they are still far away from being fully understood (Hale et al., 2020). In comparison with their larger counterparts, NP are emerging contaminants of higher concern. Additionally, they are very difficult to sample (Nguyen et al., 2019; Schwaferts et al., 2019) due to their small sizes. Furthermore, NP have a high permeation ability into human and animal tissues (Lehner et al., 2019; Wagner and Reemtsma, 2019). Recently, it was also found that submicrometer plastics and NP enter higher plants from soils and thereby potentially entering the food web via the terrestrial pathway (Li et al., 2020; Sun et al., 2020).

Recycling is considered the most sustainable and viable solution for existing plastic waste in the context of energy and fuel savings as well as reduction of CO_2 emission (Rahimi and García, 2017; Vollmer et al., 2020). Biotechnological recycling of plastics that allows the recovery of their monomer feedstocks has emerged as a promising strategy (Wei et al., 2020), especially for polyethylene terephthalate (PET) which is widely used to produce beverage bottles, food packaging and synthetic fibers (Wei and Zimmermann, 2017). A recent breakthrough published in *Nature* has showcased an efficient biocatalytic depolymerization of pretreated post-consumer PET bottles within 10 h at a pilot industrial scale (Tournier et al., 2020). Here, they used engineered variants of a plant-metagenome-derived cutinase (LC-cutinase) which showed superior thermostability and PET hydrolyzing activity at elevated temperatures compared to its mesophilic counterpart (Wei et al., 2019b), e.g. the *Ideonella sakaiensis* PETase. This PETase received a great attention by the scientific community as it was identified in a bacterium isolated at plastic recycling sites (Yoshida et al., 2016). In addition to the large quantity of PET found in the mixed plastic waste streams, its contribution to nanoplastic pollutant, usually in the form of microfibers derived from textile 'polyester', is remarkable in various aquatic systems (Deng et al., 2020; Suaria et al., 2020).

PET particles in nano- (<100 nm) and submicrometer (0.1–1 μm) range have been generated using various source materials dissolved in different solvents and dripped into water as an anti-solvent (Rodríguez-Hernández et al., 2019; Welzel et al., 2002). These artificial PET nanoparticles (PET NP) have been used to study their impact on human macrophage cells (Rodríguez-Hernández et al., 2019) and their enzymatic degradation by a wide range of polyester hydrolases and their variants (Barth et al., 2015a; Danso et al., 2018; Weber et al., 2019; Wei et al., 2014a; Wei et al., 2012; Wei et al., 2014b; Welzel et al., 2002). So far, the degradation of PET NP via the cleavage of their ester bonds, has been previously monitored indirectly, either by the release of monomeric degradation products such as terephthalic acid (Barth et al., 2015a; Wei et al., 2012) or by turbidity change of the PET NP suspension (Danso et al., 2018; Wei et al., 2014a; Wei et al., 2014b). As a consequence, the kinetic and mechanistic features on the enzymatic PET NP depolymerization have not been unambiguously elucidated.

In theory, the cleavage of the ester bond can be monitored directly and in real time via the heat production rate of the reaction (Charsley et al., 2019). Each ester bond is assigned an enthalpy value $\Delta_{EB}H$. The main advantages of calorimetric process monitoring are that the reaction progress is displayed in real time and that the measurement performance is independent of the reaction matrix, either solid such as soil, food, tissue, or liquid such as turbid suspensions, organic solvents etc. The non-biological alkaline ester hydrolysis has already been studied intensively by calorimetry (Wadsö and Karlsson, 2013). It was applied to quantify rate constants and reaction enthalpies (Skaria et al., 2005), to check the performance of custom-built calorimeter for different applications (Wadsö and Li, 2008) and is even used for calibration of isothermal microcalorimeters (Beezer et al., 2001) or flow-through calorimeters (O'Neill et al., 2003). In general, calorimetric methods were already successfully developed and tested for enzyme measurements in homogeneous mixtures as reviewed before (Bianconi, 2007). These methods provide thermodynamic data such as reaction enthalpy, heat capacity, Gibbs energy as well as rate constants and their temperature dependency using instruments with reaction vessels from the nanoliter (nL) (van Schie et al., 2018) up to the liter (L) range (Maskow and Paufler, 2015). Knowledge of the thermodynamic state variables allow in principle the prediction of the influence of environmental conditions on the NP degradation using the well-established thermodynamic framework. For instance, the van 't Hoff equation predicts the influence of temperature on reaction equilibria using the Gibbs energy and the reaction enthalpy or equations of state such as ePC-SAFT allow the prediction of the influence of the chemical environment on enzyme-catalyzed reactions (Greinert et al., 2020; Vogel et al., 2020). Isothermal titration calorimetry (ITC) has already been proven to be particularly valuable for such thermokinetic measurements when the thermal inertia of the calorimeter is taken into account (Hansen et al., 2016). The reaction in ITC is started by the addition of the reactants or the enzyme and the thermal measurement is only minimally disturbed by the addition. Todd and Gomez (2001) developed a thermokinetic method for the evaluation of the ITC data. However, their method was not designed for interfacial, heterogeneous enzymatic catalysis, which occurs during the degradation of PET NP.

Therefore, the enzymatic hydrolysis of PET NP using the thermophilic cutinase TfCut2 from *Thermobifida fusca* (Roth et al., 2014) was monitored by analytical ITC in this study. By extending established heterogeneous kinetic models for the NP degradation with a thermodynamic approach, the thermal signals could be interpreted mechanistically. The resulting thermokinetic model can help to individually analyze the adsorption behavior and the degradation performance of nanoplastics by microbial enzymes, thus enabling further understanding of the fate of nanoplastics in aquatic environments.

2. Experimental section

2.1. Preparation and characterization of PET NP

PET NP were produced according to a slightly modified protocol (Welzel et al., 2002). Briefly, 0.1 g of post-consumer PET clamshell packaging with an initial crystallinity of approximately 5–6% (Wei et al., 2019a) was dissolved in 10 mL 1,1,1,3,3,3-hexafluoro-2-propanol at room temperature for at least 12 h. This solution was dropped into 100 mL ultra-filtered water while stirring thoroughly at 13,000 rpm using an overhead stirrer. Precipitated polymer formed small particles, which can preserve as stable aqueous suspension whereas the larger aggregates were removed with a standard folded filter. The organic solvent was then removed from the particle suspension using a rotary evaporator. To determine the polymer concentration, 2 mL of suspension was centrifuged, and the resulting polymer pellet was dried at 50 °C for 24 h before the mass was determined gravimetrically. A polymer suspension containing up to 2.5 g L^{-1} of PET NP was obtained. Afterwards, nanoparticle tracking analysis (NTA) was conducted to determine the size distribution of the particles prepared this way using a NanoSight LM10 (NanoSight, Amesbury, United Kingdom), equipped with a 532 nm laser. Before acquisition, PET nanoparticles were diluted in phosphate buffered saline (PBS) to a final concentration of about 10^8–10^9 particles per mL. The measurements were performed at 25 °C. Each sample was measured at five different positions for 60 s in three independent experiments. For the capturing and analyzing of the acquired data the NTA 3.0 software was used. To better understand the fate of PET NP during enzymatic degradation, partially degraded PET NP were collected and analyzed by scanning electron microscopy (SEM), X-ray diffraction (XRD), and Fourier transform infrared spectroscopy (FTIR), as described in detail in the Supplementary Material (SM).

2.2. Production and purification of enzymes

The TfCut2-catalyzed degradation of PET NP was previously well described by a turbidimetric method (Wei et al., 2014a) and thus proved an ideal example to validate our ITC measurement in this study. The synthetic gene of the mature TfCut2 (ENA: FR727681) from *Thermobifida fusca* KW3 was purchased from Twist Bioscience (San Francisco, USA). The inactive mutant TfCut2_S130A was created by substituting the catalytic serine with an alanine residue using the Q5 Site-Directed Mutagenesis Kit (NEB, Ipswich, USA) after the manufacturer's instructions. The recombinant expression of both enzymes was carried out in *Escherichia coli* BL21(DE3) harboring pET-26b(+) vectors based on a slightly modified protocol as described previously (Roth et al., 2014). Recombinant proteins were purified using an immobilized metal affinity chromatography (IMAC) resin charged with cobalt (TALON, Takara Bio Europe SAS, Saint-Germain-en-Laye, France). Recombinant enzymes obtained in homogeneity were analyzed by SDS-PAGE and then dialyzed against 100 mM sodium phosphate buffer (pH 8.0) for storage at 4 °C prior to further use. Protein contents were determined by the Bradford method using bovine serum albumin as standard (Bradford, 1976).

2.3. Isothermal Titration Calorimetry (ITC)

The samples have to be prepared before ITC measurement. Solutions of active and inactive cutinase were originally prepared in 100 mM sodium phosphate buffer (pH 8) and the PET NP were present in water. This significant difference between both solutions must be adjusted to reduce the release of heat of dilution. Therefore, the solutions were diluted and adjusted to a buffer concentration of 12.5 mM sodium phosphate (pH 8). The calorimetric titration experiments were performed with two different types of ITC. The TAM ITC (Titration setup using the TAM IV; TA-instruments, New Castle, DE, USA) was used for the determination of the total hydrolysis enthalpy of the PET NP, whereas the PEAQ-ITC (Malvern Panalytical Ltd., Malvern, UK) was used to follow the enzymatic degradation. For the total alkaline hydrolysis of PET NP (measured by the TAM ITC), the NP suspension was diluted in 12.5 mM sodium phosphate puffer to obtain the following concentrations: 0.25, 0.65, 1.0 and 1.31 g L^{-1}. The calorimetric vessel contained 800 μL of 1 M NaOH in 12.5 mM sodium phosphate and the syringe contained 100 μL of PET NP with the different concentrations. The reference measurements were performed without PET NP in the syringe. The measurements of the total hydrolysis were carried out at 60 °C, with a stirrer speed of 80 rpm using 850 μL water in the reference cell.

For measuring the enzymatic degradation in the PEAQ-ITC, the titration cell was filled with the enzyme solution and the PET NP were in the syringe. The volume of the titration cell was 200 μL. Different concentrations of enzyme (in the range 0–0.265 g L^{-1}) and NP (in the range 0–0.221 g L^{-1}) were used in the individual experiments. The measurements were carried out at 60 °C. The following settings were used: reference power is 20 μW, high feedback, stirring speed of 750 rpm and initial delay of 900 s. Single injection measurements were recorded with one injection each with 39 μL (injection rate 0.5 μL s^{-1}) and the length of the measurement was chosen so that the signal returned to the baseline level. Three single injection measurements were carried out one after the other, in which the cell contents were not exchanged in between. These were then evaluated using ConCat 32 from Malvern Panalytical. In order to be able to calculate the heat of dilution, reference experiments were carried out. On the one hand the PET NP were titrated to buffer and on the other hand buffer was titrated to the enzyme as negative control. All measurements were performed as triple determinations.

3. Results and discussion

3.1. Thermokinetic model

A two-step enzymatic degradation mechanism of polymers has been previously proposed (Kartal and Ebenhoh, 2013; Lee et al., 2005; Mukai et al., 1993; Scandola et al., 1998; Tang and Riley, 2019) and adopted for the thermokinetic analysis of the enzymatic degradation of PET NP in this study. The list of all used symbols, their properties and units can be found in SM (Table S2). The first step of the reaction mechanism is the adsorption of the enzyme on the plastic surface (solid-liquid interface) and the second step is the cleavage of the ester bonds leading to small molecules of different molecular weights that are water-soluble. Mono- and dimeric esters of PET, such as mono(hydroxyethyl) terephthalate (MHET) and bis(hydroxyethyl) terephthalate (BHET) have been shown to inhibit the enzymatic degradation with high affinities to the active centre of the biocatalysts but less susceptible to further hydrolysis to the monomeric building blocks (Barth et al., 2015a). In comparison, the degradation monomers including terephthalic acid (TA) and ethylene glycol (EG) showed no inhibitory effect (Tournier et al., 2020). In time, both processes will overlap, with the adsorption being faster than the cleavage of the ester bonds. The principle of the total process is shown in Fig. 1.

The total heat, Q (in J L^{-1}, Eq. (1b)), and the heat production rate, $\dot{Q}$ (in W L^{-1}, Eq. (1a)), are therefore composed of the two partial contributions. The first is related to the ester cleavage reaction (Q^{EB}, $\dot{Q}^{EB}$) and the second to the adsorption of the enzyme on the NP surface (Q^{Ads}, $\dot{Q}^{Ads}$)

$$Q = Q^{EB} + Q^{Ads} = C_{EB}\cdot\Delta_{EB}H + C_E^{Ads}\cdot\Delta_{Ads}H \quad (1a)$$

$$\dot{Q} = \dot{Q}^{EB} + \dot{Q}^{Ads} = r_{EB}\cdot\Delta_{EB}H + r_E^{Ads}\cdot\Delta_{Ads}H \quad (1b)$$

C_{EB}, C_E^{Ads}, r_{EB}, r_E^{Ads}, $\Delta_{EB}H$, $\Delta_{Ads}H$ stand for the concentration of cleaved ester bonds in the NP (in mol L^{-1}), the amount of adsorbed enzyme per NP (in mol L^{-1}), the cleavage rate (in mol L^{-1} s^{-1}), the adsorption rate (in mol L^{-1} s^{-1}), the reaction enthalpy of the cleavage of the ester

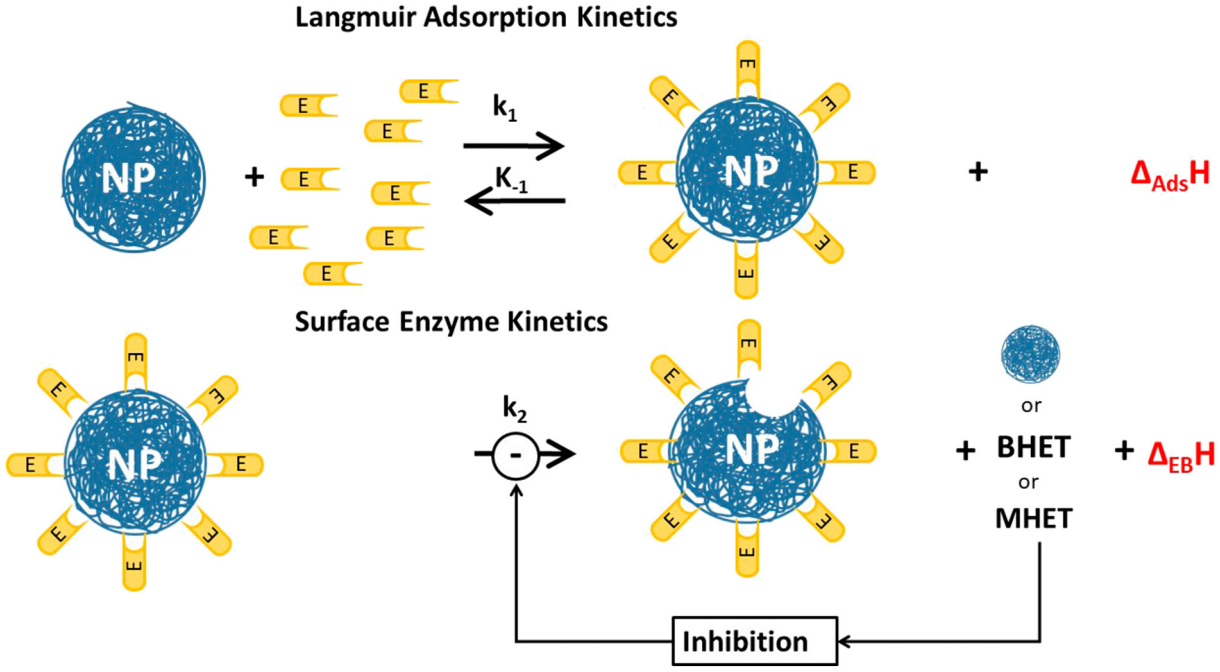

Fig. 1. Scheme of the kinetic and energetic model. k values stand for the respective kinetic constants.

bonds, (in J mol^{-1}), and the adsorption enthalpy (in J mol^{-1}), respectively. The relation between the total heat and the heat production rate is given by Eq. (2).

$$Q = \int \dot{Q}\, dt \tag{2}$$

For the separation of the two effects NP are titrated to an inactive (TfCut2_S130A) and later to an active form of TfCut2. In the first case, the contribution of the reaction term is zero. The adsorption heat can be determined by variation of C_E^{Ads} in the calorimetric vessel taking the same C_{EB} in the syringe. The number of cleaved ester bonds can be quantified if $\Delta_{EB}H$ and the adsorption contribution are known by titrating NP to the active enzyme and measuring calorimetrically the released heat. In practice, however, this heat is superimposed by thermal effects of dilution of the enzyme ($Q_{ref,\,E}(C_E)$) or the PET NP in buffer ($Q_{ref,\,NP}(C_{NP})$). Both values can be measured by titrating the enzyme C_E dissolved in buffer to the same buffer and of buffer to the PET NP C_{NP} diluted in the same buffer. Q is therefore determined by the difference between the raw data ($Q_{exp}(C_E C_{NP})$) and the reference values according to Eq. (3a). The same applies to the heat production rate $\dot{Q}$ according to Eq. (3b).

$$Q = Q_{exp}(C_E C_{NP}) - Q_{ref,NP}(C_{NP}) - Q_{ref,E}(C_E) \tag{3a}$$

$$\dot{Q} = \dot{Q}_{exp} C_E, C_{NP} - \dot{Q}_{ref,NP} C_{NP} - \dot{Q}_{ref,E} C_E \tag{3b}$$

The enthalpy of the ester cleavage $\Delta_{EB}H$ was obtained from an additional titration experiment realizing the total alkaline hydrolysis of PET under the same conditions as for the enzymatic cleavage. Here, it is assumed that the catalyst and the different pH values have only negligible influence on the reaction enthalpy. In this case, the slope of the plot of the measured heat Q_{AH} versus the total concentration of all ester bonds from the PET NPs (C_{EB}^{NP}) provides $\Delta_{EB}H$ according to Eq. (4). C_{EB}^{NP} equals the concentration of the NP, C_{NP}^0 in g L^{-1}, divided by the molar mass of the repeating unit, M = 192.17 g mol^{-1}, and the number of ester bonds per repeating unit (2).

$$Q_{AH} = Q_{ref,AH} + C_{EB}^{NP} \cdot \Delta_{EB}H \tag{4}$$

$Q_{ref,AH}$ is the heat of dilution of the buffer to the alkaline solution in the calorimetric chamber. The $\Delta_{EB}H$ obtained in this way can be used to calculate the completeness of the enzymatic PET NP degradation. For that purpose, Eq. (1a) only needs to be rearranged to Eq. (5) providing the concentration of the enzymatically cleaved ester bonds C_{EB}.

$$C_{EB} = \frac{Q^{EB} - C_E \cdot \Delta_{Ads}H}{\Delta_{EB}H} \tag{5}$$

The degree of degradation η of the NP can be calculated thereof.

$$\eta = \frac{C_{EB}}{C_{EB}^{NP}} = \frac{(Q - C_E \cdot \Delta_{Ads}H) \cdot 2 \cdot M}{\Delta_{EB}H \cdot C_{NP}^0} \tag{6}$$

The heat production rate of the cleavage process, $\dot{Q}^{EB}$, is the product of the cleavage rate of the ester bonds r_{EB} (in mol L^{-1} s^{-1}) and the enthalpy of the ester cleavage $\Delta_{EB}H$.

$$\dot{Q}^{EB} = r_{EB} \cdot \Delta_{EB}H \tag{7}$$

Kinetic models are needed to evaluate the information content of the heat production rate. There are several models describing the enzymatic or bacterial degradation of microplastics (Lee et al., 2005; Scandola et al., 1998; Tang and Riley, 2019), which can potentially be applied to PET NP degradation. For the enzymatic degradation of PET NP, in particular, both Langmuir adsorption based (Wei et al., 2014a; Wei et al., 2014b) and canonical Michaelis−Menten (M-M) analogous (Barth et al., 2015a) models have been applied for the kinetic analysis. In addition, the former model has been also applied to analyze the kinetics of enzymatic degradation of PET films and fabrics (Ronkvist et al., 2009; Silva et al., 2011). Nevertheless, the inverse M-M kinetic model has been recently shown to be more reliable for the kinetic study of heterogeneous enzymatic cellulose depolymerization, which is analogous to the enzymatic PET degradation occurring at the solid-liquid interface mostly circumventing substrate saturation (Kari et al., 2017). From the viewpoint of mathematical practice, the constant K (or K_M) derived from the inverse M-M kinetics is reciprocal to the adsorption equilibrium constant (K_A) obtained based on the Langmuir adsorption model. In

this study, we simply adopted this inverse M-M kinetic model to evaluate the enzymatic PET NP hydrolysis determined by calorimetry. A brief mathematical derivation is shown in the following.

$$E + EB \underset{k_{-1}}{\overset{k_1}{\rightleftarrows}} E/EB \tag{8}$$

$$E/EB \xrightarrow{k_2} P + E \tag{9}$$

Here E and EB are the enzyme and the substrate (ester bond), respectively. E/EB is the enzyme-substrate complex, and P represents the hydrolysis products. If a steady state for reaction 8 is assumed, the kinetic equation simplifies to Eq. (10).

$$k_1 \cdot C_E \cdot C_{EB} = k_{-1} \cdot C_{E/EB} \tag{10}$$

Assuming the adsorption of the enzyme on the surface of the NP, C_{EB} available for the enzyme is proportional to the "free" PET particle surface ($C_{EB} = a \cdot \mathcal{F} \cdot (1-\Theta)$) and $C_{E/EB}$ is proportional to the surface a (in cm^2) occupied by the enzyme $C_{E/EB} = a \cdot \mathcal{F} \cdot \Theta$. $\mathcal{F}$ is the proportionality factor. From Eq. (11) the parameter θ can be derived.

$$\theta = \frac{C_E}{(K + C_E)} \qquad \text{with} \qquad K = \frac{k_{-1}}{k_1} \tag{11}$$

For the kinetics of the hydrolysis step (9) can be written:

$$r_{EB} = \frac{d\,C_{EB}}{d\,t} = -k_2 \cdot C_{E/EB} = -k_2 \cdot \mathcal{F} \cdot a \cdot \theta = -k_2 \cdot \mathcal{F} \cdot a \cdot \frac{C_E}{(K + C_E)} \tag{12}$$

To solve the differential Eq. (12), time dependence of the particle surface, a, is needed. a is proportional to the actual concentration of PET NP. When all this is taken into account, we obtain Eq. (13) (for more details see SM).

$$r_{EB} = -\frac{C^0_{NP}}{M \cdot 2} \cdot \mathbb{C} \cdot \frac{C_E}{(K + C_E)} \cdot exp\left(-\mathbb{C} \cdot \frac{C_E}{(K + C_E)} \cdot t\right) \quad \text{with} \quad \mathbb{C} = k_2 \cdot \mathcal{F} \cdot \frac{12 \cdot M}{d_P \cdot \rho} \tag{13}$$

ρ, d_p, M stand for the density (in g m^{-3}), the mean diameter of the NP (in m) and for the molar mass of repeating unit, respectively. The molar mass of the PET repeating unit is M = 192.17 g mol^{-1}. The particle diameter d_p was determined by NTA (nanoparticle tracking analysis) to be 85 ± 6 nm parameters. This value falls in the size range of nanoplastics (< 100 nm) and is in a similar range as previously determined with PET NP derived from other material sources by dynamic light scattering ranging from 106 to 164 nm (Wei et al., 2014a). The density (ρ = 1.38 g cm^{-3}) was taken from literature (Kong and Hay, 2002). The heat production rate over time can be calculated combining Eqs. (7) and (13).

$$\dot{Q} = \Delta_{EB}H \cdot \frac{C^0_{NP}}{M \cdot 2} \cdot \mathbb{C} \cdot \frac{C_E}{K + C_E} \cdot \exp -\mathbb{C} \cdot \frac{C_E}{K + C_E} \cdot t \tag{14}$$

Eq. (14) describes a first order kinetics concerning the concentration of NP and also assumes that the concentration of the enzyme remains constant during the reaction. Thus, the slope of the logarithmic plot of the heat production rate versus time equals to $-C \cdot \frac{C_E}{(K+C_E)}$. The slope contains information on both the kinetic constant k_2 (part of $\mathbb{C}$) and the equilibrium constant K. In order to distinguish between both parameters, the heat production rate at the beginning of the PET NP degradation $\dot{Q}_0$ and the initial concentration of NP, C^0_{NP}, and the respective initial enzyme concentration, C_E, is considered (Eq. (15)).

$$\dot{Q}_0 = \Delta_{EB}H \cdot \frac{C^0_{NP}}{M \cdot 2} \cdot \mathbb{C} \cdot \frac{C_E}{K + C_E} \tag{15}$$

For that purpose, the heat production rate is extrapolated to time zero and different experiments with different amounts of PET particles and enzymes were performed. Eq. (15) predicts saturation behavior concerning the enzyme concentration C_E and allows estimating by parameter fitting the estimation of K.

Our inverse M-M-based model for the enzymatic PET NP hydrolysis predicts that i) the heat production rate should decline exponentially during each experiment, ii) the correlation of $\dot{Q}_0$ versus the concentration of the PET NP should be linear and iii) the correlation of $\dot{Q}_0$ versus the enzyme concentration should provide an M-M kinetics-like behavior. In order to validate the feasibility of our model, these predictions will be tested in the following.

3.2. Enthalpy of ester bond cleavage

The most important parameter for the thermokinetic model is the enthalpy of the ester cleavage of PET NP. This value was determined by alkaline hydrolysis of different amounts of the PET NP using ITC. The results are shown in SM (Fig. S1). The slope in the plot of the reaction heat versus the number of available ester bonds provides the enthalpy of the ester cleavage of $\Delta_{EB}H$ = – 54.1 ± 1.9 kJ mol^{-1} assuming the total hydrolysis under the given measuring conditions (pH = 14, T = 333.15 K, P = 101,325 Pa). For the cleavage of ester bonds in PET backbone no literature data are available for comparison. However, such enthalpies are known for comparable esters as summarized in Table 1. These values are very similar to the value we obtained with PET NP.

3.3. Degree of the enzymatic cleavage of ester bonds in PET NP

The reaction heat after titration of PET NP to the enzymes depends on the number of the cleaved ester bonds according to Eq. (6). Consequently, calorimetry should provide the degree of the degradation of PET NP. For this purpose, the heat production rate was integrated until the decay of the reaction, defined as the heat signal disappearing in the instrument noise (typically after 20–60 min). Indeed, the evaluation of the calorimetric experiments in this way provides an average percentage of cleaved ester bonds of 12.9 ± 2.4% based on 17 individual measurements (different concentration of NP and enzyme). At first glance, this seems surprisingly small, but it may also be due to the accessibility of the ester bonds. In other words, the enzyme works - in accordance with our model - on the surface and only very slowly makes its way to the interior of the PET NP. There is no statistically significant influence of the NP concentration on the percentage of the cleaved ester bonds (Fig. 2A). A higher ratio of the enzyme to the NP concentration, however, improves the completeness of the cleavage slightly (Fig. 2B).

A previous study (Barth et al., 2015a) has investigated the enzymatic degradation of similarly prepared PET NP at 60 °C in a thermoshaker at 1000 rpm. Based on the hydrolysis products released, a maximal degree of degradation of 60% was obtained after 60 min incubation with 50 μg mL^{-1} TfCut2 in 0.5 M Tris-HCl buffer (pH 8.5). An extension of reaction time up to 24 h did not result in significantly further degradation. In comparison with the relatively lower degradation degree determined

Table 1
Enthalpies of the cleavage of ester bonds.

Material	Enthalpy (in kJ mol^{-1})	Reference
PET	−54.1 ± 1.9	This study
PVAc	−57.3	Wadsö and Karlsson, 2013
PLA	−57.9	Wadsö and Karlsson, 2013
Methylparaben	−59.2 ± 0.4	Skaria et al., 2005
Ethylparaben	−64.4 ± 1.3	Skaria et al., 2005
Propylparaben	−60.1 ± 0.3	Skaria et al., 2005
Propylparaben	−56 ± 3	Wadsö and Li, 2008

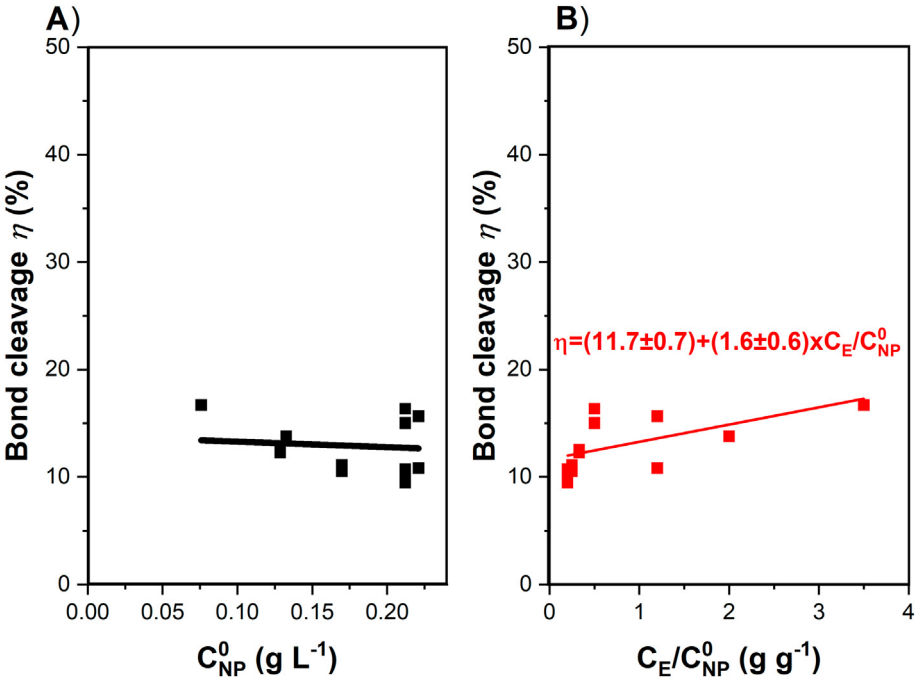

Fig. 2. Percentage of the cleavage of the enzymatic ester bonds of the PET NPs as a function of the concentration of the NP (A) and as a function of the enzyme/NP ratio (B). In A) Pearson's correlation coefficient is −0.096 and the *p*-value of the F-test is 0.712 meaning that the slope is not significant different from zero. In B) Pearson's correlation coefficient is 0.581 and the *p*-value for the F-test is 0.015 meaning that the assumed linear model is statistically different from a constant η.

in this study, higher buffer concentration as well as vigorous shaking in the former report could be considered advantageous for the enzymatic depolymerization process, consistent with the conclusions in other relevant studies using PET foils as substrates (Barth et al., 2015b; Schmidt et al., 2016). In addition, another earlier study showed an over 80% degradation of agarose-immobilized PET NP with TfCut2 (Wei et al., 2014a) after 40 min reaction at 60 °C, indicating that the use of hydrogel may also help to trap the biocatalyst on the PET NP surface thereby promoting a more effective degradation.

The inhibition of the cutinase reaction by the oligomeric cleavage products BHET and MHET may also be another reason hampering the progress of the PET NP depolymerization (Barth et al., 2015a). To test this hypothesis calorimetrically, NP were added three times in succession to a TfCut2 solution. If the hypothesis is correct, there should be little or no cleavage reaction after the second and third addition. This should be reflected by a significantly reduced heat production rate. Indeed, this behavior was observed as Fig. S2 in SM exemplarily shows. In principle, the comparison of heat curves should be suitable for testing inhibition models. However, this was not tried here because the reduction in heat production rate was so drastic that it is difficult to quantify the second and third subsequent signals from the calorimetric signal in separation. Previous studies have indicated that the enzymatic degradation of PET using TfCut2 was strongly influenced by the buffer concentration applied (Schmidt et al., 2016). As we used a lower concentration (12.5 mM) of phosphate buffer for the ITC investigation, a moderate degradation rate and degree was expected. Both FTIR and XRD analysis of partially degraded PET NP (see SM) indicated an increase in crystallinity during the enzymatic degradation, similarly to what has been described previously (Wei et al., 2019a). The increased crystallinity of PET NP deteriorates its biodegradability, leading to incomplete degradation, as we observed under the prevailing conditions.

3.4. Enthalpy contributions of ester bond cleavage and adsorption

The recombinant mature TfCut2 used in this study was expressed in *E. coli* harboring a pET-26(+) vector which confers a C-terminal His_6-tag to the recombinant enzyme resulting in a molecular mass of 29.3 kDa. Fig. 3 compares the reaction heat of the enzymatic NP hydrolysis with active and inactive TfCut2. The reaction heat of PET NP degradation is exothermic and two orders of magnitude greater than the adsorption heat of the enzyme on the PET NP, which is endothermic. In contrast to the hyperbolic shape with the active enzyme, the inactive enzyme showed an apparently linear shape. That is surprising, because surface adsorption processes show usually a saturation behavior. A linear relation, however, would be expected when the added enzyme binds completely to the PET NP surface. Under this circumstance, the slope of 4.3 ± 0.5 J g^{-1} allows the estimation of the adsorption enthalpy $\Delta_{Ads}H = 126 \pm 15$ kJ mol^{-1} according to Eq. (1a). Literature data on the enthalpy of the adsorption of enzymes or proteins on nanoplastics for

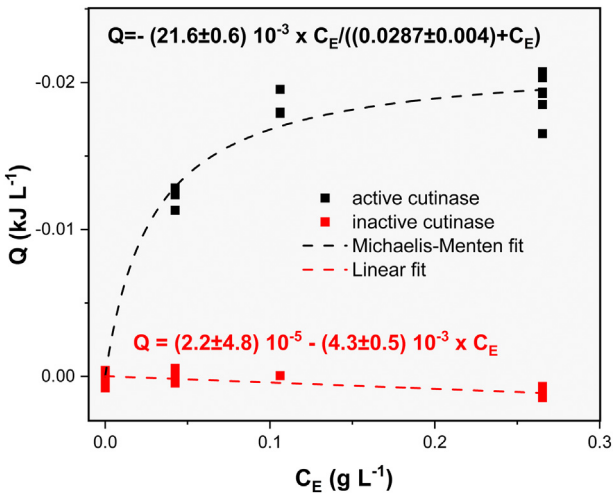

Fig. 3. Reaction heat as a function of the amount of enzyme for $C^0_{NP} = 0.215$ g L^{-1}. If the saturation behavior of the reaction heat (active cutinase) is described by an inverse M-M kinetic function, a maximum heat of −0.0216 ± 0.0006 J L^{-1}, a K_m value of 0.0287 ± 0.0039 g L^{-1}, and a *p*-value of the F-test of 10^{-35} is obtained. For the adsorption process (inactive cutinase) Pearson's correlation coefficient of −0.807 and the *p*-value of the F-test of $3 \cdot 10^{-11}$ is obtained assuming a linear model.

comparison do not exist to our knowledge. Treating bovine serum albumin (BSA) in the same manner an adsorption enthalpy of – 1.12 ± 0.42 J g^{-1} or - 74 ± 25 kJ mol^{-1} (M = 66,000 g mol^{-1}) is obtained, and the slope is significantly different from zero at 0.05 level (see Fig. S3 in SM). Nevertheless, in order to get an idea of the magnitude of the expected adsorption enthalpy the SM contains adsorption enthalpies of different enzymes and proteins on different surfaces (Table S3 in SM). These values vary between −40 and 50 kJ mol^{-1} and are therefore at least in the order of magnitude of our values. A good review about the interaction forces between synthetic particles and biomacromolecules, that can give us an imagination why the variance of the adsorption enthalpies is so large, was published previously (Hoshino et al., 2014). The other approximation to the observed linear relationship is the consideration of the maximum loading of the nanoparticles with the enzyme. Unfortunately, there are also no measurements of nanoparticles available in literature. However, Zumstein et al. (2016) have investigated the adsorption of a lipase on various polyester thin films including PET by quartz crystal microbalance with dissipation monitoring (QCM-D), and indicated the highest affinity of PET to the enzyme with adsorbed mass up to 12 μg cm^{-2}. Based on the size and concentration of PET NP used in this study, this value corresponds to an enzyme concentration of 1.21 g L^{-1}. This value is between four and five times higher than our maximum enzyme concentration (0.27 g L^{-1}). Because no data on TfCut2 are available in literature, other model proteins are also considered. The adsorption of model protein (BSA) on thin films of 8 different polymers (unfortunately without PET) was measured using a static adsorption method by Wang and Shi (2010) and modelled by Fang et al. (2019) providing maximum adsorbed mass between 3.89 and 28.52 μg cm^{-2}. These values correspond to enzyme concentration between 0.17 and 2.5 g L^{-1} which makes our measurement below the maximum load with enzyme probable and could explain our observation of a linear correlation.

The corrected reaction heat showed a saturation behavior (Fig. 3) which seems to be understandable knowing that only a very small part of the ester bonds was cleaved. As long as only a few enzyme molecules are present, each additional molecule contributes to the cleavage until the cleavage limit is reached. At high enzyme concentrations, however, the cleavage limit is exceeded and the additional dosage of enzyme molecules do not contribute.

3.5. Verification of the model predictions

The next important question is whether the new thermokinetic model can describe the experiments and which kinetic parameters we can expect at which accuracy. The comparison of the predictions with the experiment is shown visually in Fig. 4 and quantitatively in Table 2.

Eq. (14) can be simplified as Eq. (16).

$$\dot{Q}=\dot{Q}_0\cdot\exp(-b\cdot t) \quad \text{with} \quad \dot{Q}_0 = \frac{\Delta_{EB}H\cdot C\cdot C^0_{NP}}{2\cdot M}\cdot\frac{C_E}{(K+C_E)} \quad \text{and} \quad b = C\cdot\frac{C_E}{(K+C_E)} \tag{16}$$

Dividing the parameter $\dot{Q}_o$ by b and plotting versus the start concentration of the NP, C^0_{NP}, should show a linear correlation and the slope should provide the enthalpy of the ester bond cleavage according to Eq. (17). For the parameter fitting to Eq. (16) to obtain $\dot{Q}_0$ the first 100 s of signal was not considered because this part is influenced by the thermal inertia of the instrument (Hansen et al., 2016).

$$\frac{\dot{Q}_0}{b} = \frac{\Delta_{EB}H}{2\cdot M}\cdot C^0_{NP} \tag{17}$$

From the slope (−169 ± 24 J g^{-1}) the enthalpy of the ester cleavage of $\Delta_{EB}H = -64.9 \pm 9.2$ kJ mol^{-1} can be derived which statistically

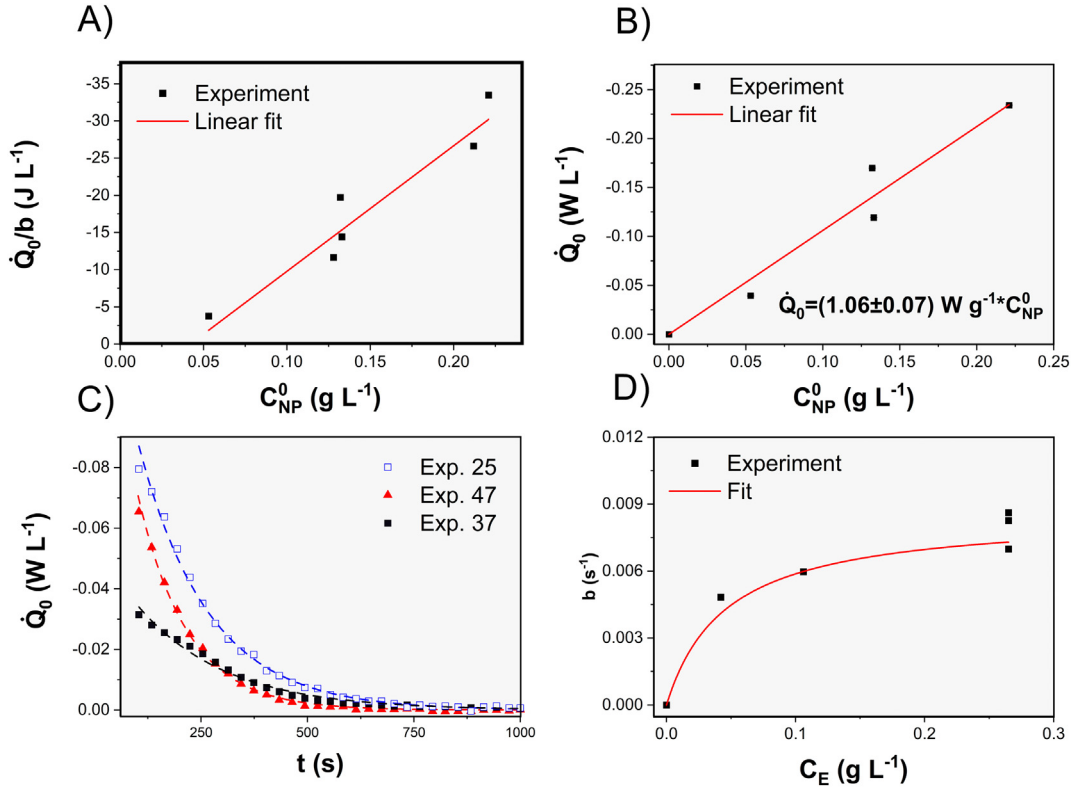

Fig. 4. Thermokinetic evaluation of the decay of the heat production rate after addition of PET NP to TfCut2. A): Verification of the predicted linear correlation according to Eq. (17); B): Verification of the predicted linear correlation between $\dot{Q}_0$ and the concentration of NP for a constant enzyme concentration C_E = 0.265 g L^{-1} according to Eq. (17); C) Verification of the predicted exponential decay of the heat signal after injection of different amounts of NP to enzyme according to Eq. (14) (values are given in Table 2); D) Verification of the predicted saturation behavior according to Eq. (16).

Table 2
Comparison of predictions using Eq. (14) and derivative thereof explained in the following with experimental data.

Predictions		Experiment		
	Limiting condition	Shown in	Quantitative (P, p)[a]	Derived parameter
Linear relation: $\frac{Q_0}{b}$ vs. C^0_{NP}	None	Fig. 4A	P = 0.962 p = 0.00211	$\Delta_{EB}H = -64.9 \pm 9.2$ kJ mol^{-1}
Linear relation: $\dot{Q}_0$ vs. C^0_{NP}	C_E = const.	Fig. 4B	P = 0.991 p = 0.0001	None
Exponential drop: $\dot{Q}_0$ vs. t	None	Fig. 4C	P = N/A $p < 10^{-14}$[b]	Table S4 in SM
Saturation behavior: b vs. C_E	None	Fig. 4D	P = N/A $p = 7 \cdot 10^{-7}$	$\Delta_{EB}H = -48.4 \pm 10.4$ kJ mol^{-1} K = 0.046 ± 0.015 g L^{-1} $\mathbb{C}$ = 0.00856 ± 0.0008 s^{-1}

[a] P-Pearson's correlation coefficient; p- probability of the zero hypothesis in the F-Test.
[b] Exemplarily given for experiment 25.

corresponds to the value of the alkaline cleavage (-54.1 ± 1.9 kJ mol^{-1}). The b-parameter of Eq. (16) is predicted to show a saturation behavior, which is indeed observed experimentally (Fig. 4D). The fitting parameter $\mathbb{C}$ and K can be applied to estimate $\Delta_{EB}H = -48.4 \pm 10.4$ kJ mol^{-1} according to Eq. (16). The relatively large error of 20% is because erroneous values are included in the calculation. The maximum error estimation is described in Section 8 in SM. The error contributions are 43% for $\mathbb{C}$, 31% for the slope and 26% for K, respectively. Even this third enthalpy corresponds statistically to the other two, confirming our model. Eq. (14) predicts an exponential drop of the heat signal in accordance with the experiments (Fig. 4C) and the derived parameter are exemplarily given in Table S4 in SM.

Here we determined an adsorption-equilibrium associated constant K = 0.046 ± 0.015 g L^{-1} by ITC. This value is quantitatively in a good agreement with various previous studies, e.g. K = 0.031 g L^{-1} and 0.039 g L^{-1} obtained by turbidimetric analysis of the TfCut2-catalyzed agarose-immobilized PET NP prepared from amorphous PET films and PET fibers, respectively (Wei et al., 2014a), and K = 0.06 g L^{-1} calculated based on the release of degradation products determined from the enzymatic hydrolysis of PET fabrics using Tfu_0883, an enzyme highly homologous (sharing 99% sequence identity) to TfCut2 (Silva et al., 2011). These results validate our ITC measurements as well as its applicability in the quantitative analysis of the enzymatic nanoplastic degradation.

3.6. Degradation pattern of the PET nanoparticles

A further criterion for the NP degradation is the change in the size distribution after the reaction. This was quantified by NTA and is shown in Fig. 5.

At the beginning of the reaction the size distribution of PET NP is with a modal value of 85 ± 6 nm relatively narrow and the particles are very uniform. This value is in good agreement with the similarly prepared PET NP size in the range of 106–164 nm determined by dynamic light scattering shown in a previous study (Wei et al., 2014a). In comparison to the PET NP prepared in a different manner (Rodríguez-Hernández et al., 2019) with a more broad size distribution from 50 to 300 nm, PET NP derived by our procedure has a more uniform size distribution. During the enzymatic degradation, the proportion of particles with the initial size distribution decreases considerably as expected. After 5 days almost all material of this particle size has disappeared seemingly in contradiction to the relatively low degree of degradation of the data obtained from the ITC measurement. The apparent

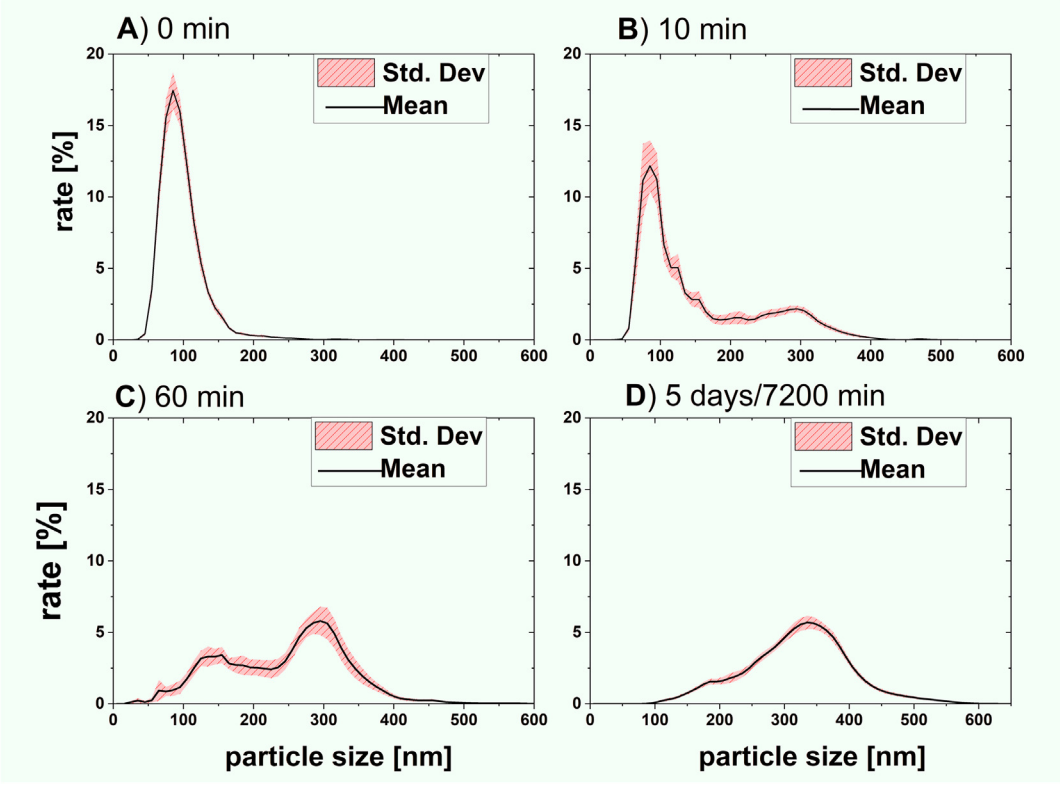

Fig. 5. Changes in the size distribution of PET NP as a function of the duration of the enzymatic degradation. A): Size distribution of untreated NPs with a modal size of 85 ± 6 nm. B): Size distribution of NPs degraded by enzymes for 10 min. These particles showed multimodal distribution with a major fraction at size of 85 ± 3 nm. C): Size distribution of NP degraded by enzymes for 60 min. The modal value was shifted to 220 ± 27 nm. D): After 5 days of enzymatic treatment the modal size of the particles was finally shifted to 330 ± 7 nm.

contradiction is resolved because the ITC monitor the cleavage of ester bonds, whereas the NTA measures the formation of aggregates that still contain many ester bonds. This explanation is supported by the formation of large agglomerates with a broad size distribution. The enzymatic degradation is assumed to alter the surface charge and homogeneity of the nanoparticle suspension and thus causing agglomeration upon long-term incubation. This assumption is supported by the SEM analysis of the partially degraded PET NP and NP incubated in plain buffer (see Fig. S4 in SM). Agglomeration of PET NP was observed in both samples, but reduced particle size was seen only in PET NP after enzymatic treatment.

3.7. Concluding evaluation of the ITC method and the thermokinetic model

Calorimetry has the advantages i) to provide kinetic and stoichiometric information in real-time, ii) no need for complex and elaborated analytics, iii) to combine adsorption with chemical reactions, iii) to operate even in complex matrices, and iv) to provide thermodynamic state variables which allow predictions applying the thermodynamic framework. In principle, the time course of the reaction heat (heat production rate) is also suited for testing mechanistic models of the nanoparticle degradation. This was shown using the example of a well-known two-phase mechanistic kinetic model for the PET NP degradation (Lee et al., 2005; Scandola et al., 1998; Tang and Riley, 2019; Wei et al., 2014a; Wei et al., 2014b) in combination with a thermodynamic approach. The first phase is the adsorption of the enzyme on the surface of the PET NP and the second phase is the actual cleavage of the ester bonds. All predictions of the model were experimentally validated illuminating the potential of calorimetry for testing mechanistic kinetic models. The model predicts different correlations that provide independent thermodynamic and kinetic parameters ($K = 0.046 \pm 0.015$ g L^{-1}, $\mathbb{C}$=0.0056 ± 0.0008 s^{-1}). As an example, the enthalpy of cleaving the ester bonds was quantified i) using the alkaline hydrolysis ($\Delta_{EB}H = -54.1 \pm 1.9$ kJ mol^{-1}), ii) using the signal decay after adding PET NP to TfCut2 according to Eq. (17) ($\Delta_{EB}H = -64.9 \pm 9.2$ kJ mol^{-1}) or iii) evaluating the saturation behavior of the b-parameter according to Eq. (16) ($\Delta_{EB}H = -48.4 \pm 10.4$ kJ mol^{-1}). These values cannot be distinguished statistically which suggests the correctness of the proposed thermokinetic model. The heat production of PET NP degradation is determined to about 95% by the heat of reaction and only to 5% by the heat of adsorption, which is clearly shown by the comparison of the reaction with active and inactive cutinase. The predictive power of our model is tested by comparing the predictions with the experiments (Fig. 6). The slope in Fig. 6 is 0.993 ± 0.028 (expected is 1.00) and Pearson's correlation coefficient is 0.993 which indicates the suitability of our model in the investigated range.

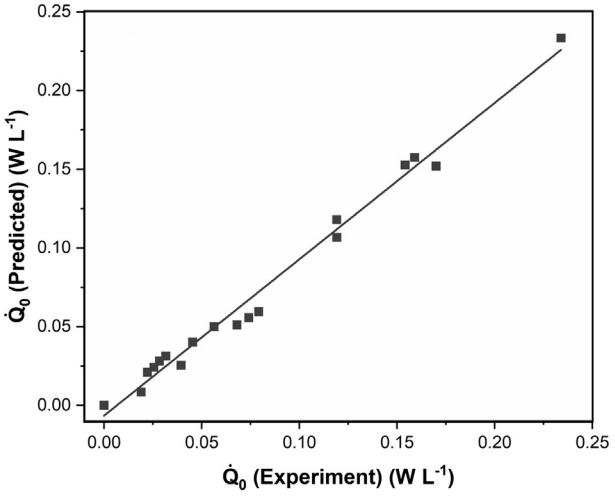

Fig. 6. Comparison of 19 experimental and predicted $\dot{Q}_0$ values. The probability of the F-test is $1.8 \cdot 10^{-17}$.

4. Conclusion

This is the first time that we have direct real-time access to the enzymatic cleavage of ester bonds in PET NP via calorimetry. The proposed measurement method and model are perfectly suited to screen for efficient biocatalysts for NP degradation and to quantify the most important key figures in a simple way. Since the type of catalyst used is irrelevant for calorimetry and thermodynamics, the method should be equally suitable for all types of biocatalysts including whole-cell plastic degrading catalysts like bacteria (Yan et al., 2020) and fungi. The fact that the new method provides a state variable $\Delta_{EB}H$ and an equilibrium constant K can be used in the further development of the method to make predictions on the influence of environmental conditions (e.g. temperature, chemical composition of the environment) on PET NP degradation based on the well-established thermodynamic framework. In addition, the method might be suitable for the analysis of other enzymatically decomposable polymeric NP. However, this will require many more investigations after this demonstration of the principle. Motivating for the further development of this research approach is the fact that highly sensitive calorimeters with sub-nanowatt resolution are currently being developed (Hur et al., 2020).

CRediT authorship contribution statement

Kristina Vogel: Formal analysis, Investigation, Data curation, Visualization. **Ren Wei**: Conceptualization, Resources, Project administration, Funding acquisition. **Lara Pfaff**: Investigation, Resources. **Daniel Breite**: XRD SEM FTIR investigation, data evaluation and text preparation. **Hassan Al-Fathi**: Investigation. **Christian Ortmann**: Formal analysis. **Irina Estrela-Lopis**: Investigation, Visualization. **Tom Venus**: Investigation, Visualization. **Agnes Schulze**: Supervision. **Hauke Harms**: Supervision. **Uwe Bornscheuer**: Supervision. **Thomas Maskow**: Conceptualization, Methodology, Writing –original draft. **All authors**: Writing-review & editing, Validation.

Declaration of competing interest

The authors declare that they have no known competing financial interests or personal relationships that could have appeared to influence the work reported in this paper.

Acknowledgements

The authors gratefully acknowledge the support of this work by the German Science Foundation (DFG) grant No. MA 3746/6-1 and by the European Union's Horizon 2020 research and innovation programme (grant number 870294; MIX UP project). Hassan Al-Fathi is thankful for supporting his work by the Philipp Schwarz-initiative. The authors would like to thank the analytical team at the Leibniz Institute of Surface Engineering (IOM) (Jan Griebel, Andrea Prager and Nadja Schönherr) for their help with the analysis of PET NP (SEM, IR, XRD).

Appendix A. Supplementary material

Supplementary data to this article can be found online at https://doi.org/10.1016/j.scitotenv.2021.145111.

References

Barth, M., Oeser, T., Wei, R., Then, J., Schmidt, J., Zimmermann, W., 2015a. Effect of hydrolysis products on the enzymatic degradation of polyethylene terephthalate nanoparticles by a polyester hydrolase from *Thermobifida fusca*. Biochem. Eng. J. 93, 222–228.

Barth, M., Wei, R., Oeser, T., Then, J., Schmidt, J., Wohlgemuth, F., et al., 2015b. Enzymatic hydrolysis of polyethylene terephthalate films in an ultrafiltration membrane reactor. J. Membr. Sci. 494, 182–187.
Beezer, A.E., Hills, A.K., O'Neill, M.A.A., Morris, A.C., Kierstan, K.T.E., Deal, R.M., et al., 2001. The imidazole catalysed hydrolysis of triacetin: an inter-and intra-laboratory development of a test reaction for isothermal heat conduction microcalorimeters used for determination of both thermodynamic and kinetic parameters. Thermochim. Acta 380, 13–17.
Bianconi, M.L., 2007. Calorimetry of enzyme-catalyzed reactions. Biophys. Chem. 126, 59–64.
Bradford, M.M., 1976. A rapid and sensitive method for the quantitation of microgram quantities of protein utilizing the principle of protein-dye binding. Anal. Biochem. 72, 248–254.
Charsley, E., Price, D., Hunter, N., Gabbott, P., Kett, V., Gaisford, S., et al., 2019. Principles of Thermal Analysis and Calorimetry: R. Soc. Chem. .
Danso, D., Schmeisser, C., Chow, J., Zimmermann, W., Wei, R., Leggewie, C., et al., 2018. New insights into the function and global distribution of polyethylene terephthalate (PET)-degrading bacteria and enzymes in marine and terrestrial metagenomes. Appl. Environ. Microb. 84, e02773–17.
Dawson, A.L., Kawaguchi, S., King, C.K., Townsend, K.A., King, R., Huston, W.M., et al., 2018. Turning microplastics into nanoplastics through digestive fragmentation by Antarctic krill. Nat. Commun. 9, 1001.
Deng, H., Wei, R., Luo, W., Hu, L., Li, B., Shi, H., 2020. Microplastic pollution in water and sediment in a textile industrial area. Environ. Pollut. 258, 113658.
Fang, L., Singh, R., Waxman, L., Zhao, C., 2019. Model protein adsorption on polymers explained by Hansen solubility parameters. J. Pharm. Sci. 108, 187–192.
Geyer, R., Jambeck, J.R., Law, K.L., 2017. Production, use, and fate of all plastics ever made. Sci. Adv. 3, e1700782.
Greinert, T., Vogel, K., Seifert, A.I., Siewert, R., Andreeva, I.V., Verevkin, S.P., et al., 2020. Standard Gibbs energy of metabolic reactions: V. enolase reaction. Biochim. Biophys. Acta Proteins Proteom. 1868, 140365.
Hale, R.C., Seeley, M.E., La Guardia, M.J., Mai, L., Zeng, E.Y., 2020. A global perspective on microplastics. J. Geophys. Res. Oceans 125 e2018JC014719.
Hansen, L.D., Transtrum, M.K., Quinn, C., Demarse, N., 2016. Enzyme-catalyzed and binding reaction kinetics determined by titration calorimetry. Biochim. Biophys. Acta 1860, 957–966.
Hoshino, Y., Lee, H., Miura, Y., 2014. Interaction between synthetic particles and biomacromolecules: fundamental study of nonspecific interaction and design of nanoparticles that recognize target molecules. Polym. J. 46, 537–545.
Hur, S., Mittapally, R., Yadlapalli, S., Reddy, P., Meyhofer, E., 2020. Sub-nanowatt resolution direct calorimetry for probing real-time metabolic activity of individual *C. elegans* worms. Nat. Commun. 11, 2983.
Jambeck, J.R., Geyer, R., Wilcox, C., Siegler, T.R., Perryman, M., Andrady, A., et al., 2015. Plastic waste inputs from land into the ocean. Science 347, 768–771.
Kari, J., Andersen, M., Borch, K., Westh, P., 2017. An inverse Michaelis-Menten approach for interfacial enzyme kinetics. ACS Catal. 7, 4904–4914.
Kartal, O., Ebenhoh, O., 2013. A generic rate law for surface-active enzymes. FEBS Lett. 587, 2882–2890.
Kong, Y., Hay, J.N., 2002. The measurement of crystalinity of polymers by DSC. Polymer 43, 3873–3878.
Lebreton, L.C., Van Der Zwet, J., Damsteeg, J.-W., Slat, B., Andrady, A., Reisser, J., 2017. River plastic emissions to the world's oceans. Nat. Commun. 8, 15611.
Lee, H.J., Wark, A.W., Goodrich, T.T., 2005. Surface enzyme kinetics for biopolymer microarrays: a combination of Langmuir and Michaelis-Menten concepts. Langmuir 21, 4050–4057.
Lehner, R., Weder, C., Petri-Fink, A., Rothen-Rutishauser, B., 2019. Emergence of nanoplastic in the environment and possible impact on human health. Environ. Sci. Technol. 53, 1748–1765.
Li, L., Luo, Y., Li, R., Zhou, Q., Peijnenburg, W.J.G.M., Yin, N., et al., 2020. Effective uptake of submicrometre plastics by crop plants via a crack-entry mode. Nat. Sustain. 3, 929–937.
Maskow, T., Paufler, S., 2015. What does calorimetry and thermodynamics of living cells tell us? Methods 76, 3–10.
Mukai, K., Yamada, K., Doi, Y., 1993. Kinetics and mechanism of heterogeneous hydrolysis of poly[(R)-3-hydroxybutyrate] film by PHA depolymerase. Int. J. Biol. Macromol. 15, 362–366.
Nguyen, B., Claveau-Mallet, D., Hernandez, L.M., Xu, E.G., Farner, J.M., Tufenkji, N., 2019. Separation and analysis of microplastics and nanoplastics in complex environmental samples. Acc. Chem. Res. 52, 858–866.
O'Neill, M., Beezer, A.E., Labetoulle, C., Nicolaides, L., Mitchell, D.A., Orchard, J.A., et al., 2003. The base catalysed hydrolysis of methyl paraben: a test reaction for flow microcalorimeters used for determination of both kinetic and thermodynamic parameters. Thermochim. Acta 399, 63–71.
PlasticsEurope, 2019. Plastics – the Facts. PlasticsEurope https://www.plasticseurope.org/de/resources/publications/2154-plastics-facts-2019.
Rahimi, A., García, J.M., 2017. Chemical recycling of waste plastics for new materials production. Nat. Rev. Chem. 1, 0046.
Rochman, C., Browne, M.A., Halpern, B.S., Hentschel, B.T., Hoh, E., Karapanagioti, H.K., et al., 2013. Classify plastic waste as hazardous. Nature 494, 169–171.
Rodríguez-Hernández, A.G., Muñoz-Tabares, J.A., Aguilar-Guzmán, J.C., Vazquez-Duhalt, R., 2019. A novel and simple method for polyethylene terephthalate (PET) nanoparticle production. Environ. Sci. Nano 6, 2031–2036.
Ronkvist, Å.M., Xie, W., Lu, W., Gross, R.A., 2009. Cutinase-catalyzed hydrolysis of poly (ethylene terephthalate). Macromolecules 42, 5128–5138.
Roth, C., Wei, R., Oeser, T., Then, J., Follner, C., Zimmermann, W., et al., 2014. Structural and functional studies on a thermostable polyethylene terephthalate degrading hydrolase from *Thermobifida fusca*. Appl. Microbiol. Biotechnol. 98, 7815–7823.
Scandola, M., Focarete, M.L., Frisoni, G., 1998. Simple kinetic model for the heterogeneous enzymatic hydrolysis of natural poly(3-hydroxybutyrate). Macromolecules 31, 3846–3851.
Schmidt, J., Wei, R., Oeser, T., Belisário-Ferrari, M.R., Barth, M., Then, J., et al., 2016. Effect of Tris, MOPS, and phosphate buffers on the hydrolysis of polyethylene terephthalate films by polyester hydrolases. FEBS Open Bio 6, 919–927.
Schwaferts, C., Niessner, R., Elsner, M., Ivleva, N.P., 2019. Methods for the analysis of submicrometer- and nanoplastic particles in the environment. Trends Analyt. Chem. 112, 52–65.
Silva, C., Da, S., Silva, N., Matama, T., Araujo, R., Martins, M., et al., 2011. Engineered *Thermobifida fusca* cutinase with increased activity on polyester substrates. Biotechnol. J. 6, 1230–1239.
Skaria, C.V., Gaisford, S., O'Neill, M.A.A., Buckton, G., Beezer, A.E., 2005. Stability assessment of pharmaceuticals by isothermal calorimetry: two component systems. Int. J. Pharm. 292, 127–135.
Suaria, G., Achtypi, A., Perold, V., Lee, J.R., Pierucci, A., Bornman, T.G., et al., 2020. Microfibres in oceanic surface waters: a global characterization. Sci. Adv. 6, eaay8493.
Sun, X.D., Yuan, X.D., Jia, Y., et al., 2020. Differentially charged nanoplastics demonstrate distinct accumulation in *Arabidopsis thaliana*. Nat. Nanotechnol. 15, 755–760.
Tang, J., Riley, W.J., 2019. Competitor and substrate sizes and diffusion together define enzymatic depolymerization and microbial substrate uptake rates. Soil Biol. Biochem. 139, 107624.
Todd, M., Gomez, E., 2001. Enzyme kinetics determined using calorimetry: a general assay for enzyme activity? Anal. Biochem. 296, 179–187.
Tournier, V., Topham, C.M., Gilles, A., David, B., Folgoas, C., Moya-Leclair, E., et al., 2020. An engineered PET depolymerase to break down and recycle plastic bottles. Nature 580, 216–219.
van Schie, M., Ebrahimi, K.H., Hagen, W.R., Hagedoorn, P.L., 2018. Fast and accurate enzyme activity measurements using a chip-based microfluidic calorimeter. Anal. Biochem. 544, 57–63.
Vogel, K., Greinert, T., Harms, H., Sadowski, G., Held, C., Maskow, T., 2020. Influence of cytosolic conditions on the reaction equilibrium and the reaction enthalpy of the enolase reaction accessed by calorimetry and van 't HOFF. Biochim. Biophys. Acta Gen. Subj. 1864, 129675.
Vollmer, I., Jenks, M.J.F., Roelands, M.C.P., White, R.J., van Harmelen, T., de Wild, P., et al., 2020. Beyond mechanical recycling: giving new life to plastic waste. Angew. Chem. Int. Ed. 59, 15402–15423.
Wadsö, L., Karlsson, O.J., 2013. Alkaline hydrolysis of polymers with ester groups studied by isothermal calorimetry. Polym. Degrad. Stab. 98, 73–78.
Wadsö, L., Li, X., 2008. A simple rate law experiment using a custum-built isothermal heat conduction calorimeter. J. Chem. Educ. 85, 112–116.
Wagner, S., Reemtsma, T., 2019. Things we know and don't know about nanoplastic in the environment. Nat. Nanotechnol. 14, 300–301.
Wang, B., Shi, B., 2010. Comparison of surface tension components and Hansen solubility parameters theories. Part I: explanation of protein adsorption on polymers. J. Macromol. Sci. B 49, 383–391.
Weber, J., Petrovic, D., Strodel, B., Smits, S.H.J., Kolkenbrock, S., Leggewie, C., et al., 2019. Interaction of carbohydrate-binding modules with poly(ethylene terephthalate). Appl. Microbiol. Biotechnol. 103, 4801–4812.
Wei, R., Zimmermann, W., 2017. Biocatalysis as a green route for recycling the recalcitrant plastic polyethylene terephthalate. Microb. Biotechnol. 10, 1302–1307.
Wei, R., Oeser, T., Billig, S., Zimmermann, W., 2012. A high-throughput assay for enzymatic polyester hydrolysis activity by fluorimetric detection. Biotechnol. J. 7, 1517–1521.
Wei, R., Oeser, T., Barth, M., Weigl, N., Lübs, A., Schulz-Siegmund, M., et al., 2014a. Turbidimetric analysis of the enzymatic hydrolysis of polyethylene terephthalate nanoparticles. J. Mol. Catal. B Enzym. 103, 72–78.
Wei, R., Oeser, T., Then, J., Kühn, N., Barth, M., Schmidt, J., et al., 2014b. Functional characterization and structural modeling of synthetic polyester-degrading hydrolases from *Thermomonospora curvata*. AMB Express 4, 44.
Wei, R., Breite, D., Song, C., Grasing, D., Ploss, T., Hille, P., et al., 2019a. Biocatalytic degradation efficiency of postconsumer polyethylene terephthalate packaging determined by their polymer microstructures. Adv. Sci. 6, 1900491.
Wei, R., Song, C., Grasing, D., Schneider, T., Bielytskyi, P., Bottcher, D., et al., 2019b. Conformational fitting of a flexible oligomeric substrate does not explain the enzymatic PET degradation. Nat. Commun. 10, 5581.
Wei, R., Tiso, T., Bertling, J., O'Connor, K., Blank, L.M., Bornscheuer, U.T., 2020. Possibilities and limitations of biotechnological plastic degradation and recycling. Nat. Catal. 3, 867–871.
Welzel, K., Müller, R.-J., Deckwer, W.D., 2002. Enzymatischer Abbau von polyesternanopartikeln. Chem. Ing. Tech. 74, 1496–1500.
Worm, B., Lotze, H.K., Jubinville, I., Wilcox, C., Jambeck, J., 2017. Plastic as a persistent marine pollutant. Annu. Rev. Environ. Resour. 42, 1–26.
Wright, S.L., Kelly, F.J., 2017. Plastic and human health: a micro issue? Environ. Sci. Technol. 51, 6634–6647.
Yan, F., Wei, R., Cui, Q., Bornscheuer, U.T., Liu, Y.J., 2020. Thermophilic whole-cell degradation of polyethylene terephthalate using engineered *Clostridium thermocellum*. Microb. Biotechnol. https://doi.org/10.1111/1751-7915.13580.
Yoshida, S., Hiraga, K., Takehana, T., Taniguchi, I., Yamaji, H., Maeda, Y., et al., 2016. A bacterium that degrades and assimilates poly(ethylene terephthalate). Science 351, 1196–1199.
Zumstein, M.T., Kohler, H.P., McNeill, K., Sander, M., 2016. Enzymatic hydrolysis of polyester thin films: real-time analysis of film mass changes and dissipation dynamics. Environ. Sci. Technol. 50, 197–206.